Journal of Mammalian Evolution

https://doi.org/10.1007/s10914-021-09541-0

Accepted: 8 March 2021

Morphometric analysis of the mandible of primitive sabertoothed felids from the late Miocene of Spain

Short title: Morphometric analysis of early sabertoothed felids

Narimane Chatar[1,*], Valentin Fischer[1], Gema Siliceo[2], Mauricio Antón[2], Jorge Morales[2], and Manuel J. Salesa[2]

[1] Evolution and Diversity Dynamics Lab, Université de Liège, Belgium

[2] Departamento de Paleobiología, Museo Nacional de Ciencias Naturales-CSIC, C/José Gutiérrez Abascal, 2. 28006 Madrid, Spain

* Corresponding author: narimane.chatar@uliege.be

ABSTRACT

How sabertoothed felids have evolved their iconic morphology remains unclear because of the patchy fossil record of early machairodontines. Batallones localities in the Madrid region (Spain) have the potential to clarify this as two sites have yielded hundreds of fossils of the early machairodontines *Promegantereon ogygia* and *Machairodus aphanistus*. Previous analyses suggested that these two sites are not contemporaneous and a morphological drift between cavities was described for these two species; characterizing intraspecific variability is thus important to better understand the evolution of machairodontines. To tackle this issue, we modelled 62 felid mandibles in 3D using a laser scanner. We applied 3D geometric morphometrics (3D GM) and linear morphometrics on these models to test for differences in populations and to better characterize the morphology of early machairodontines. Both linear measurements and 3D data reveal an absence of morphological changes in mandible shape between the two sites. Batallones machairodontines are closer to felines than to other, more derived machairodontines in mandibular morphology, suggesting the existence of rapid shift in the mandibular shape between primitive and derived members of the clade. Our analysis did

not reveal any allometric relationship between the overall shape of the mandible when studied with 3D GM and body size. Finally, we reveal a previously overlooked diversity in felid mandibular condyles, with machairodontines having much larger and medially inclined condyles.

Key words: Batallones – Felidae – geometric morphometrics – *Machairodus* – *Promegantereon*

Declarations

Funding (information that explains whether and by whom the research was supported)

NC is supported by a grant of Fonds de la Recherche Scientifique F.R.S.–FNRS (FRIA grant number FC 36251). VF is supported by a grant of Fonds de la Recherche Scientifique F.R.S.–FNRS (MIS F.4511.19). This study is part of the research projects CGL2015-68333-P (MINECO/FEDER, UE) and 201730I085 (CSIC). JM and MJS are members of the Research Group CSIC 641538 (Museo Nacional de Ciencias Naturales-CSIC, Madrid, Spain); also, MJS is a member of the Research Group FOCONTUR (Fundación Conjunto Paleontológico de Teruel-Dinópolis).

Conflicts of interest/Competing interests (include appropriate disclosures)

The authors declare that they have no conflict of interest.

Ethics approval (include appropriate approvals or waivers)

'Not applicable'

Consent to participate (include appropriate statements)

'Not applicable'

Consent for publication (include appropriate statements)

'Not applicable'

Availability of data and material (data transparency)

Tables are available as ESM 2 and ESM3. PTS files are available as ESM5 and three-dimensional surface scan are available in the MorphoSource repository (https://www.morphosource.org/dashboard/collections/000344367/) on reasonable request.

Code availability (software application or custom code)

The R script used for the analysis is available as ESM4.

ACKNOWLEDGEMENTS

NC is supported by a grant of Fonds de la Recherche Scientifique F.R.S.–FNRS (FRIA grant number FRIA FC 36251). VF is supported by a grant of Fonds de la Recherche Scientifique F.R.S.–FNRS (MIS F.4511.19). This study is part of the research projects CGL2015-68333-P (MINECO/FEDER, UE) and 201730I085 (CSIC). JM and MJS are members of the Research Group CSIC 641538 (Museo Nacional de Ciencias Naturales-CSIC, Madrid, Spain); also, MJS is member of the Research Group FOCONTUR (Fundación Conjunto Paleontológico de Teruel-Dinópolis, Spain). We would like to thank Ángel Luis Garvia (Museo Nacional de Ciencias Naturales-CSIC, Spain) and Dr Juan Francisco Pastor (Universidad de Valladolid, Spain) for kindly loaning the specimens used for comparison, and the government of the Comunidad de Madrid (Spain) for providing funding for the excavations at Cerro de los Batallones sites. For access to the surface scan data of *Dinofelis barlowi*, we thank the Ditsong National Museum of Natural History, South Africa, and Dr. Justin Adams of the Department of Anatomy and Developmental Biology, Monash University, Australia. For sharing the 3D models of *Lynx rufus* and *Puma concolor* we thank respectively the WitmerLab at Ohio University and the Illinois State Museum (USA). Also, we thank Prof. Jack Tseng and his colleagues for sharing models of *Smilodon fatalis* and *Panthera pardus*; the collection of which was funded by the National Science Foundation (DEB-1257572) and the American Museum of Natural History Frick Postdoctoral Fellowships. All these files were downloaded from www.MorphoSource.org, Duke University. Finally, we thank the editors Dr. John Wible, and Dr. Darin Croft as well as our two reviewers Dr. Michael Morlo and Dr. Camille Grohé for their helpful and constructive comments on an earlier version of this paper.

INTRODUCTION

Cerro de los Batallones is a fossiliferous complex from the late Miocene in the Madrid Region (Spain) exposing a large amount of well-preserved bones in nine pseudo-karstic cavities (Morales et al. 1992; Calvo et al. 2013) (Fig. 1). These cavities are interpreted as natural traps (Morales et al. 2000, 2008) containing what is now regarded as one of the richest Neogene fossil associations of Europe, notably for carnivorans (Morales et al. 2008). Carnivorans usually have a scarce fossil record (Eisenberg 1981; White et al. 1984) which is why Batallones-1 and Batallones-3 (two of the cavities of the Batallones complex) have drawn considerable attention since the discovery of the former in the 90's, preserving thousands of carnivoran fossils (Morales et al. 2008). Among these carnivorans, two primitive sabertoothed felids, the puma-sized *Promegantereon ogygia* and the much larger, tiger-sized *Machairodus aphanistus,* are particularly abundant in both Batallones-1 and Batallones-3 (Antón et al. 2004; Salesa et al. 2006; Monescillo et al. 2014; Siliceo et al. 2014). These taxa are currently regarded as early representatives of the clade Machairodontinae (Salesa et al. 2003, 2005, 2010a; Antón et al. 2004).

While the fossil assemblage in Batallones indicates a late Miocene age for the nine cavities (Morales et al. 2008), all these traps might not be contemporaneous (Morales et al. 2008; López-Antoñanzas et al. 2010). This assumption is supported by differences in the faunal assemblages and varying morphology of a series of taxa (López-Antoñanzas et al. 2010; Salesa et al. 2010a, 2012a; Morales et al. 2008; Monescillo et al. 2014; Siliceo et al. 2014). Siliceo et al. (2014) and Monescillo et al. (2014) noted some significant differences among both machairodontines between Batallones-1 and Batallones-3 based on selected measurements. However, there is no quantitative study comparing *Pr. ogygia* and *Ma. aphanistus* to their relatives, and differences in feeding ecology between these two primitive species and derived machairodontines has only been discussed qualitatively (Salesa et al. 2003, 2005, 2006, 2010b; Antón et al. 2004, 2020). Indeed, analyses of machairodontine mandibular morphology have poorly sampled early machairodontines, often comparing the derived *Smilodon* with other felids (Slater and Van Valkenburgh 2009; Prevosti et al. 2010; Christiansen 2012; Christiansen and Harris 2012; Piras et al. 2013, 2018; Meachen et al. 2014). The first goal of the present study is to compare the two machairodontines from Batallones-1 and Batallones-3 using three-dimensional geometric morphometrics (3D GM) and linear morphometrics in order to test the existence of a morphological shift between these two sites regarding the mandibular morphology. Results obtained with geometric morphometrics and linear morphometry will be confronted to compare the difference of signal captured by these two methods. We will thus analyse the intraspecific and

geographic/temporal variability of *Pr. ogygia* and *Ma. aphanistus* as well as their morphospace occupation compared to that of other extinct and extant felids.

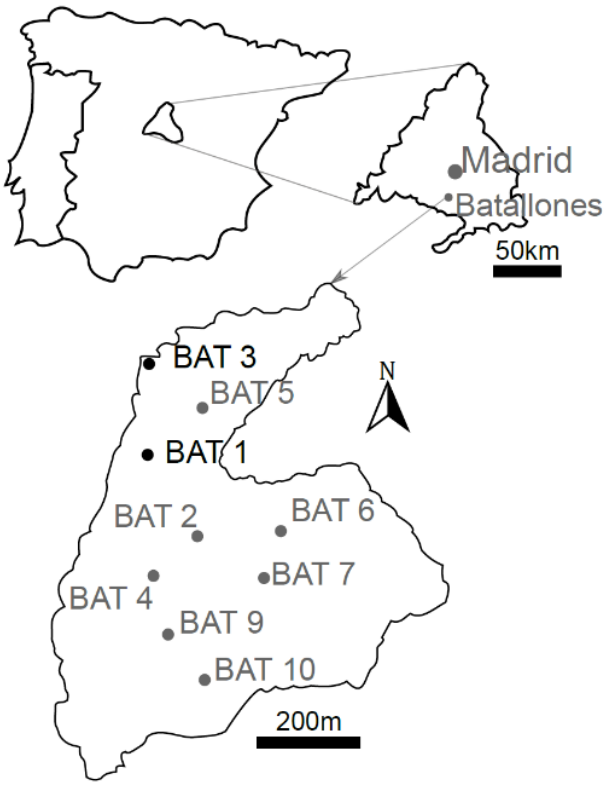

***Figure 1**: Location of the Batallones fossil sites within the Iberian Peninsula. Carnivoran-rich fossil sites are indicated in black (BAT 1 and BAT 3).*

MATERIAL AND METHODS

Material

We surface scanned 28 specimens of *Pr. ogygia* and 17 specimens of *Ma. aphanistus* housed in the collections of the Museo Nacional de Ciencias Naturales-CSIC (Madrid, Spain) using a Next Engine 3D laser surface scanner at 0.4mm resolution. Among these 45 specimens from Batallones, 12 were already studied in 2014 by Siliceo et al. (2014) and Monescillo et al. (2014) and are highlighted in bold in Table 1. Four casts of machairodontine mandibles (*Amphimachairodus giganteus* from the late Miocene of China, *Megantereon* sp. from the late Miocene of China, *Homotherium crenatidens* from the Pliocene of China, and *Xenosmilus hodsonae* from the Pleistocene of Haile limestone quarries) and eight mandibles of extant felines (*Acinonyx jubatus*, *Caracal caracal*, *Felis lybica*, *Neofelis nebulosa*, *Panthera leo*, *Panthera onca*, *Panthera tigris*, and *Panthera uncia*) housed in the collections of the Museo Nacional de Ciencias Naturales-CSIC and the Museo Anatómico de la Universidad de Valladolid (Spain) were also scanned for comparisons. All extant specimens come from zoos: the Valwo Zoo of Matapozuelos (Valladolid) for the jaguar (*Pa. onca*) and the caracal (*C. caracal*), and the Zoo Aquarium of Madrid for the others. The casts of *Am. giganteus*, *Megantereon* sp., *H. crenatidens*, and *X. hodsonae* were made on fossils housed in a private institute, the Babiarz Institute of Paleontological Studies, but the casts themselves belong to the Palaeontological collections of the MNCN-CSIC. Two other machairodontines (*Smilodon fatalis,* from the Pleistocene of Rancho La Brea, and *Dinofelis barlowi,* from the Pleistocene of South Africa) (media M7786, Tseng et al. 2016 and media M5913, Adams et al. 2015, respectively), as well as for three other felines (*Pa. pardus*: media M7779, Tseng et al. 2016, *Puma concolor*: media M8227 [Unpublished specimen] and *Lynx rufus*: media M36728 [Unpublished

specimen]) were extracted from MorphoSource. The dataset hence contains 62 specimens (Table 1) including those that were studied by Siliceo et al. (2014) and Monescillo et al. (2014) (see Table 1). When both hemimandibles were present (symphysis still fused or not), only the best-preserved one was selected for the analysis, and some of the models were therefore mirrored to compare only right hemimandibles.

***Table 1**: Material list. Institutional abbreviation: AMNH: American Museum of Natural History, DNMN: Ditsong National Museum of Natural History, ISM: Illinois state museum, MAV: Museo Anatómico de Valladolid, MNCN: Museo Nacional de Ciencias, Naturales.*

Subfamily	Taxon	Specimen n°	Age	Holding institution
Machairodontinae	*Pr. ogygia*	B-5264	Late Miocene	MNCN
	Pr. ogygia	B-7042	Late Miocene	MNCN
	Pr. ogygia	B-751	Late Miocene	MNCN
	Pr. ogygia	B-3109	Late Miocene	MNCN
	Pr. ogygia	B-134	Late Miocene	MNCN
	Pr. ogygia	B-462	Late Miocene	MNCN
	Pr. ogygia	B-5198	Late Miocene	MNCN
	Pr. ogygia	B-732	Late Miocene	MNCN
	Pr. ogygia	B-2376	Late Miocene	MNCN
	Pr. ogygia	B-4708	Late Miocene	MNCN
	Pr. ogygia	BAT-1'01 E5-17	Late Miocene	MNCN
	Pr. ogygia	BAT-1'02 E7-66	Late Miocene	MNCN
	Pr. ogygia	BAT-1'04 E4-115	Late Miocene	MNCN
	Pr. ogygia	BAT-1'05 D8-755	Late Miocene	MNCN
	Pr. ogygia	BAT-1'07 E5-97	Late Miocene	MNCN
	Pr. ogygia	BAT-1'07 E5-102	Late Miocene	MNCN
	Pr. ogygia	BAT-3'09 207	Late Miocene	MNCN
	Pr. ogygia	BAT-3'09 1250	Late Miocene	MNCN
	Pr. ogygia	BAT-3'09 779	Late Miocene	MNCN
	Pr. ogygia	**BAT-3'10 1773**	Late Miocene	MNCN
	Pr. ogygia	**BAT-3'11 132**	Late Miocene	MNCN
	Pr. ogygia	BAT-3'11 1144	Late Miocene	MNCN
	Pr. ogygia	**BAT-3'11 2020**	Late Miocene	MNCN
	Pr. ogygia	BAT-3'11 2339	Late Miocene	MNCN
	Pr. ogygia	BAT-3'13 1596	Late Miocene	MNCN
	Pr. ogygia	BAT-3'13 2070	Late Miocene	MNCN
	Pr. ogygia	BAT-3'13 2057	Late Miocene	MNCN
	Pr. ogygia	BAT-3'14 94	Late Miocene	MNCN
	Ma. aphanistus	**B-2230**	Late Miocene	MNCN
	Ma. aphanistus	**B-3974**	Late Miocene	MNCN
	Ma. aphanistus	**B-382**	Late Miocene	MNCN
	Ma. aphanistus	**B-8630**	Late Miocene	MNCN
	Ma. aphanistus	BAT-1'01 E7-82	Late Miocene	MNCN
	Ma. aphanistus	**BAT-1'04 F6-130**	Late Miocene	MNCN
	Ma. aphanistus	BAT-1'05 E6-42	Late Miocene	MNCN
	Ma. aphanistus	**BAT-1'05 F6-265**	Late Miocene	MNCN
	Ma. aphanistus	**BAT-1'06 F8-80**	Late Miocene	MNCN
	Ma. aphanistus	BAT-1'06 E4-52	Late Miocene	MNCN
	Ma. aphanistus	BAT-3'07 672	Late Miocene	MNCN

	Ma. aphanistus	BAT-3'07 698	Late Miocene	MNCN
	Ma. aphanistus	**BAT-3'08 252**	Late Miocene	MNCN
	Ma. aphanistus	**BAT-3'09 1017**	Late Miocene	MNCN
	Ma. aphanistus	BAT-3'09 1344	Late Miocene	MNCN
	Ma. aphanistus	BAT-3'11 970a	Late Miocene	MNCN
	Ma. aphanistus	BAT-3'13 1916b	Late Miocene	MNCN
	Am. giganteus	BC-102	Late Miocene	MNCN
	S. fatalis	M7786-9732	Late Pleistocene	AMNH
	Me. Sp. Indet.	CB-20	Late Miocene	MNCN
	X. hodsonae	BC-113	Pleistocene	MNCN
	D. barlowi	M5913	Pleistocene	DNMNH
	H. crenatidens	CB-06	Early Pliocene	MNCN
Felinae	*Pa. leo*	MNCN COMP-255	Actual	MNCN
	Pa. tigris	MNCN COMP-999	Actual	MNCN
	Pa. uncia	BC-56	Actual	MNCN
	Pa. pardus	AMNH 113745	Actual	AMNH
	Pa. onca	MAV-2415	Actual	MNCN
	Pu. concolor	ISM-ZOO 693928	Actual	ISM
	L. rufus	OUVC 9576	Actual	OU
	Ac. jubatus	MNCN-COMP 3438	Actual	MNCN
	C. caracal	MAV-1518	Actual	MNCN
	F. lybica	MAV-965	Actual	MNCN
	N. nebulosa	BC-005	Actual	MNCN

Three dimensional geometric morphometrics

Raw surface scan data were treated with ScanStudio (NextEngine Company, 2012) and Meshlab (Cignoni et al. 2008) to produce three-dimensional models. Out of the 62 individuals studied, 47 of them (11 felines, 17 *Pr. ogygia*, 13 *Ma. aphanistus,* and six other machairodontines) were well preserved enough to be suitable for 3D geometric morphometrics. We placed 12 type-II landmarks (Bookstein 1997) on these models using the free software Landmark editor v.3 (Wiley et al. 2005) (see Table S1 for the description of each landmark used). We added a total of 26 sliding semi-landmarks on the coronoid process (9), the mandibular diastema between the canine and the most anterior premolar (9), and along the ventral surface of the symphysis and dentary (8) (Fig. 2). Landmark coordinates were saved as .pts files which can be easily imported in R with the read.pts function of the Morpho package (Schlager 2017). All subsequent analyses were run in the R statistical environment version 3.6.0 (R Foundation for statistical computing 2019). Each file was stored as a matrix and all the specimens were assembled in a 3D array by means of the bindArr function of the Morpho package (Schlager 2017) whose role is specifically to concatenate distinct 3D files in one single array. The define.sliders function of the geomorph package (Adams et al. 2013) allows to define which points in the matrix created on the basis of the .pts files have to be considered as sliding landmarks (semi-landmarks). We applied a generalized Procrustes superimposition (Rohlf and Slice 1990) using the gpagen function of the geomorph package (Adams et al. 2013).

We computed a PCA (Principal component analysis) on the Procrustes coordinates following the protocol proposed by Polly (2013). Shapes for extreme values on the first two PCs were obtained using the plotTangentSpace R function so morphological traits which play a role in the variation can be assessed. As allometry can affect bone shape and thus influence the results of morphometrics analyses (Klingenberg 1996, 2016), we performed linear regressions between the different PCs of our PCA and the log10-transformed centroid size of our Procrustes coordinates. The dispRity package (Guillerme 2018) was used to quantify the intraspecific variability based on these Procrustes coordinates. The geomorph.ordination function was used to obtain an ordination matrix based on the geomorph.data.frame object containing shape data. As disparity measurements are influenced by the sampling (Butler et al. 2012), Guillerme (2018) suggested bootstrapping the data using the boot.matrix function from the extReme package (Gilleland and Katz 2016). The function custom.subsets from the dispRity package (Guillerme 2018) was then used to divide the two data frames depending on the site. To compare the two sites, the data were bootstrapped 1000 times for specimens from Batallones-1 and 1000 times for

specimens from Batallones-3. The metric used to calculate the total disparity was the sum of variances. A Wilcoxon test was performed with the wilcox.test function to test the difference of bootstrapped disparity between sites. The p-values obtained with wilcox.test are supposed to be less than 0.05 if the medians are significantly different, but p-values obtained with this test tend to be often very low (due to the high number of bootstraps).

Then, the function procD.lm from the geomorph package (Adams et al. 2013) was used to perform a Procrustes ANOVA on the 3D GM data to search more deeply for any differences between the two sites.

Linear morphometrics

We took nine measurements (Fig. 3, Table S2, S3) on the 62 specimens using a digital calliper, recording distances to the nearest 0.01 mm. Only the ML and CPC1L measurements for the largest species (*Ma. aphanistus*, *Am. giganteus*, *H. crenatidens*, *Pa. leo* and *Pa. tigris*) were taken using a larger, non-digital caliper, recording distance up to the nearest 0.02 mm. For the individuals for which only the 3D model was available (*S. fatalis*, *D. barlowi*, *Pu. concolor*, *Pa. pardus* and *L. rufus*) the measurements were taken using the Meshlab software. In addition, the presence/absence and development of p2 and p3 were represented using binary characters: a character for the absence or presence of p2, another for the p3, and a last one for the development of p2, which can be vestigial or not if present. Even when present, the p2 was not taken into account in the CTL measurement. The list of characters and measurements is available in Table S2. To account for the effect of size, ten ratios were computed; both the ratios and discrete variables are available in Table S3.

This mixed dataset containing the ratios and discrete characters was then scaled (z-transform), and a distance matrix based on pairwise dissimilarities was computed from this scaled dataset using the daisy function from the cluster package (Meachler et al. 2011), by means of the gower distance metric, which is ideal for datasets mixing continuous and discrete values (Gower 1971). A permutational multivariate analysis of variance (PERMANOVA, formerly “nonparametric manova” (Anderson 2001)) was performed using the adonis2 function from the vegan package (Dixon 2003) on the distance matrix to assess the difference between sites with 1000 permutations using the “gower” method. A cluster dendrogram analysis was performed with the hclust function and a principal coordinate analysis (PCoA) was computed on this distance matrix using the pcoa function from the ape package (Paradis et al. 2004). To assess the role of each ratio and variable, the envfit function from the vegan package (Dixon 2003) was used to assess the influences of each ratios and categorical data on the principal coordinates (Table 2).

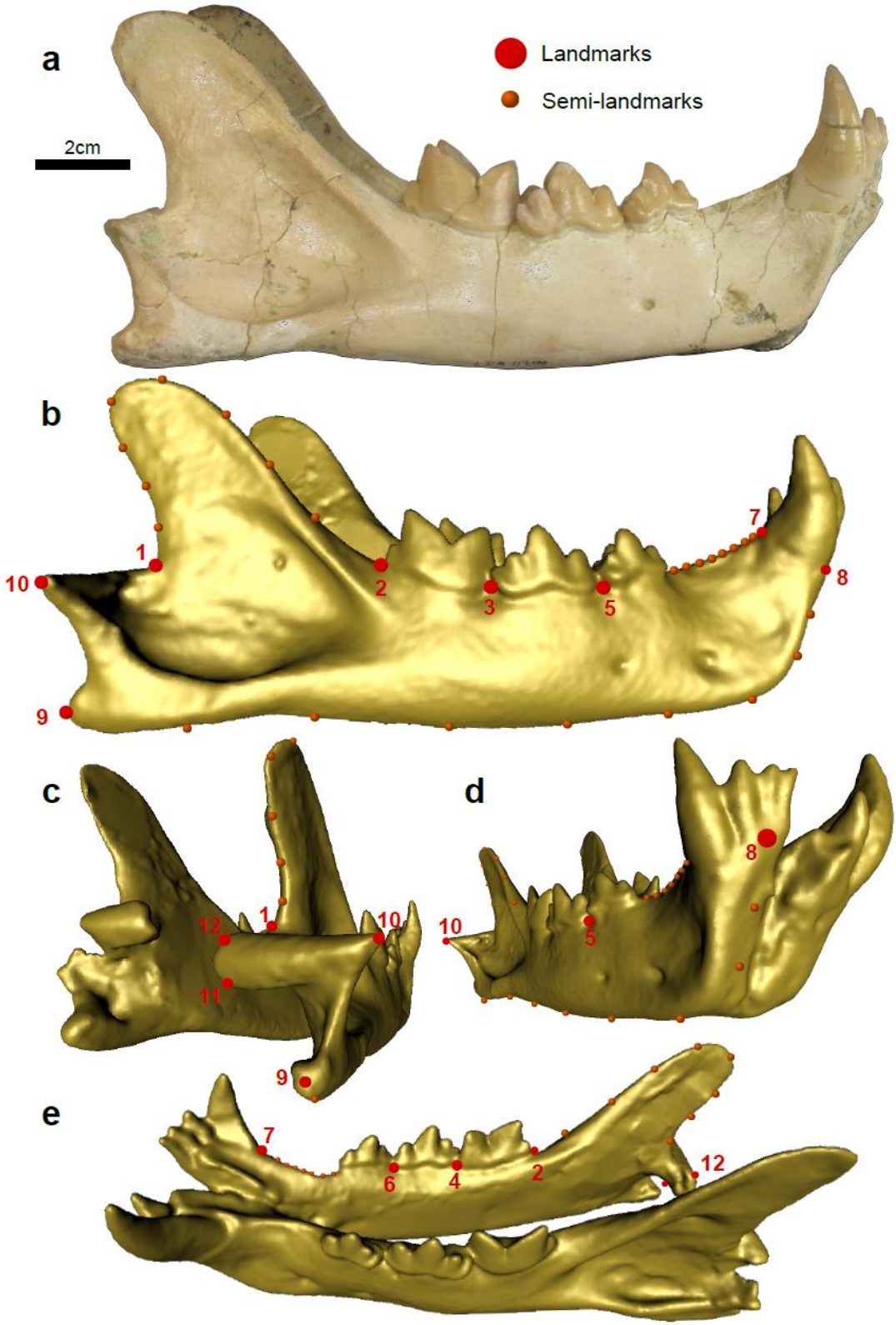

***Figure 2**: Fossil and 3D model of BAT-3'13 1916b (Ma. aphanistus), showing the landmarks and semi-landmarks used on each specimen. a: lateral view of the fossil. b, c, d, e: 3D model in lateral, caudolateral, rostrolateral, and dorsomedial views. See Table S1 for the description of each landmark used in this work*

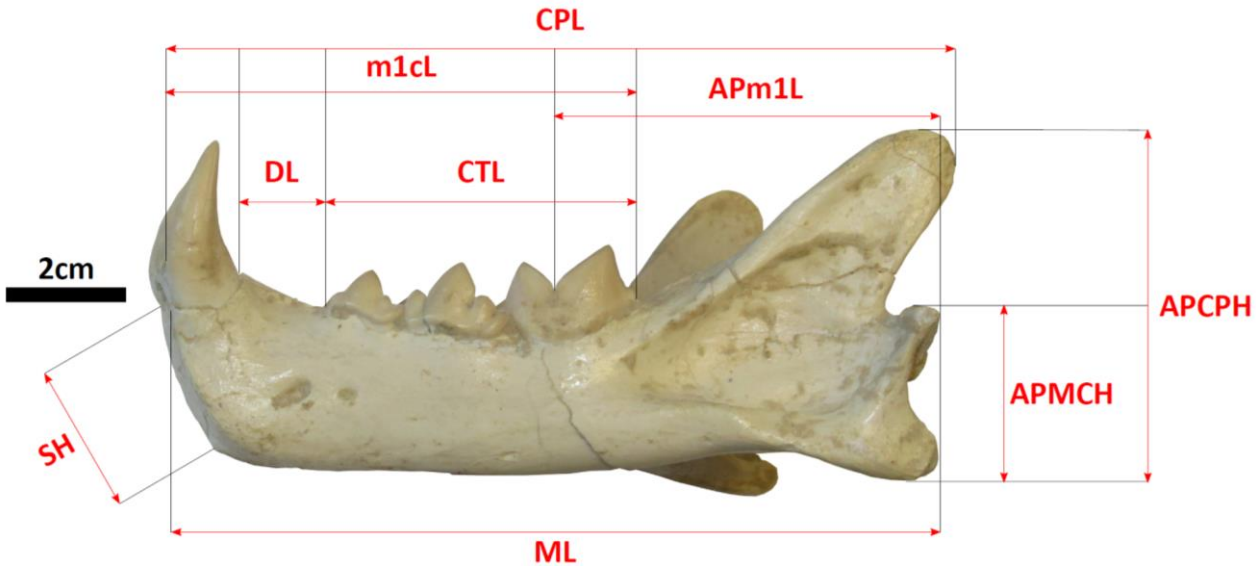

***Figure 3**: Lateral view of BAT-1'02 E7-66 (Pr. ogygia), showing the linear measurements taken on each specimen. Abbreviations: ML: mandibular length; APMCH: angular process to mandibular condyle, height; APCPH: angular process to coronoid process, height; APM1L: angular process to the notch between the protoconid and paraconid of m1, length; CPC1L: length from the coronoid process to the canine; CTL: cheek teeth length; M1CL: m1 to canine , length; DL: diastema length; SH: symphyseal height.*

Table 2: Influences of each variables on the PCoA (on the Batallones sample) first two axes given by envfit function. Variables with a significant p-value for the regressions (under a 0.05 threshold) are marked in bold.

	Axis 1	Axis 2	R^2	p-value
p2	**-0.90505**	**-0.42531**	**0.9580**	**0.001**
CPc1L/ML	0.16427	0.98642	0.2708	0.054
CTL/m1cL	**-0.61507**	**0.78847**	**0.3387**	**0.037**
(m1cL-DL-CTL)/M1CL	**-0.20824**	**0.97808**	**0.4447**	**0.007**
DL/(DL+CTL)	**0.33512**	**-0.94218**	**0.9164**	**0.001**
m1CL/ML	-0.57149	0.82061	0.2307	0.131

APm1L/ML	-0.61533	0.78827	0.1685	0.218
APCPH /ML	-0.99378	0.11134	0.0191	0.851
APMCH/APCPH	-0.55264	0.83342	0.0607	0.587
DL/ML	**0.34476**	**-0.93869**	**0.7161**	**0.001**
SH/ML	-0.39954	0.91671	0.0657	0.559

This second morphometry dataset does not rely on geometric morphometrics and thus captures a slightly different signal than the one created by 3D GM. This dataset will be used to get an estimate of the sensitivity of the results (in terms of morphospace occupation and disparity) and to test for possible differences in the two approaches (3D GM vs linear morphometry). Variability between sites was assessed by dividing the dataframe in two: one for *Pr. ogygia* and the other for *Ma. aphanistus*. Again, the function custom.subsets from the dispRity package (Guillerme 2018) was used to divide the two dataframes depending on the site. Then, another disparity analysis was run to compare the intraspecific variation in the mandibular shape of *Pr. ogygia* and *Ma. aphanistus* by taking the whole dataset and defining the subset according to the species. A distribution of the total disparity values was calculated as the sum of variances along each axis of the PCoA, for each bootstrap.

To assess if the dissimilarities among the specimens in the two dimensions ordination plot (PCoA) reflect the original dissimilarities, a non-metric multidimensional scaling (NMDS) analysis was performed using the metaMDS function and the shepard diagram was plotted using the stressplot function of the vegan package (Dixon 2003).

A mantel test was performed using the ape package (Paradis et al. 2004) to compare the results obtained in linear and three-dimensional morphometry. Mantel's permutation tests for similarity between two pairwise distances, correlations, or similarity matrices. We used the gower distance metric for the 2D dataset (as this metric is best suited for dataset mixing continuous and discrete characters) and Euclidean distances for the 3D dataset.

Data availability statement

The fossil and extant material used for this study is housed in the MNCN (Museo Nacional de Ciencias Naturales, Madrid, Spain). All the three-dimensional surface scans are available on request in the MorphoSource repository (https://www.morphosource.org/dashboard/collections/000344367/).

Supplementary figures and tables are available in ESM1. The dataset for 2D linear morphometry (Raw measurements

and ratios) are available in ESM2 and ESM3, respetively. The R script is available in ESM4. Pts files (3D Points File) containing the landmark coordinates used for analyses are available in ESM5.

RESULTS OF THE MORPHOMETRIC ANALYSIS

Morphospace occupation of *Promegantereon ogygia* and *Machairodus aphanistus* among felids

Our principal component analysis on the whole sample (felines + machairodontines) recovered 46 axes, with the first two accounting for 54.81% of the total shape variation (Fig. 4a). The first PC explains almost half of the variation (46.41%) and slightly less than a tenth for the second one (8.4%). It seems evident that the sample is well differentiated along the PC1, where felines show negative values and derived machairodontines show positive ones. Our linear regressions did not show any strong influence of the centroid size of our Procustes coordinates and any of the 46 PCs of our PCA (Table S4); R^2 values for correlation with PC1 and PC2 were 0.13 and -0.017, respectively. To make sure that some 'groups' were not more influenced by allometry we also computed distinct regressions for each group on the two first PCs but none of these groups exhibits an alometric relation between the size and shape of the mandible (Fig. S1) Interestingly, *Ma. aphanistus* and *Pr. ogygia* occupy an intermediate position between felines and derived machairodontines, but closer and partially overlapping with felines. For the PC1, specimens with greater positive values exhibit a shortened and straightened coronoid process, a straightened ventral border of the dentary, a reinforced (longer and straighter) symphysis region, and a longer diastema (sometimes due to the loss of p3). The use of 3D landmarks allowed the digitalization of the mandibular condyle, the process that articulates with the squamosal bone. It appears that the variation of size of this process plays a role in the PC1 being larger for positive values, and so, for more recent machairodontines (Fig. 4c). The orientation is also variable, being inclined towards the lingual side in felines, and towards the labial side among machairodontines (Fig. 4c). The highest loadings of Procrustes coordinates on PC1 were placed on: the diastema, the coronoid process, the ventral line of the mandible and symphysis region, the mandibular condyle, the angular process while the landmarks placed around alveoli of the teeth had the lowest loadings. The mandibular condyle does not show the highest loadings but has still higher ones than the angular process while this latter is often discussed in machairodontine diagnosis (e.g., Cooke 1991; Palmqvist et al. 2007; Antón et al. 2004, 2014; Monescillo et al. 2014). Felines and derived machairodontines completely overlap on the PC2 but this axis separated *Pr. ogygia* and *Ma. aphanistus* from the rest of the dataset. In terms of loadings, the alveoli of the teeth have more weight than in the PC1 (in a decreasing order: diastema and alveolus

of i3, coronoid process, alveoli of cheek teeth, ventral line of the mandible, mandibular condyle, and angular process). The PCoA ordination on all the specimens (Fig. 4b) recovered 25 axes with the first two axes explaining respectively 48.04% and 26.74%. The presence/absence of p3 or p2, CPCL/ML, CTL/m1cL, DL/(DL+CTL), APm1L/ML, APCPH/ML, APMCH/APCPH, and DL/ML, are the variables that were considered as tightly linked to the position of each specimen on the PCoA axis (Table 3). Axis 1 values increase with the lack of p3 (but also with the presence of a vestigial one), short cheek teeth length compared to the mandible size (low CTL/ML) but also compared to the total length occupied by the teeth (low CTL/m1cL), a reduced mesiodistal lower canine length ((m1cL-DL-CTL)/m1cL), an increased distance between the angular process and the mandibular condyle (high APMCH/APCPH), a longer diastema in comparison to the mandible length (high DL/ML) and a higher symphysis (high SH/ML). With the exception of the height between the angular process and the mandibular condyle, all these characteristics are considered as derived machairodontines features (Kurtén 1952; Emerson and Radinsky 1980; Martin 1980; Radinsky and Emerson 1982; Miller 1984, Akersten 1985; Turner and Antón 1997), which is why highly derived genera such as *Smilodon*, *Homotherium*, and *Megantereon* occupy high positive values on the first axis, while lowest values are occupied by *Pr. ogygia*, *Ma. Aphanistus*, and felines. *Panthera tigris*, *Pa. pardus,* and *N. nebulosa* are the felines with the highest values on the first axis, and thus the closest to the machairodontines and especially to *Am. giganteus* on that axis.

Figure 4*:Patterns of morphospace occupation. a, b: morphospace occupation of modern felines and machairodontines. a: first two axes of the PCA using the 3D procrustes coordinates (PCA). b: first two axes of the PCoA using 2D morphometry data. c: representation Representation of extreme values on PC1 in caudal view showing the difference in size and orientation of the mandibular condyle. d, e: per species and per site differences for the Batallones taxa Pr. ogygia and Ma. aphanistus. d: First two axes of the PCA using the 3D landmark coordinates (PCA). e: First two axes of the PCoA using 2D morphometry data.*

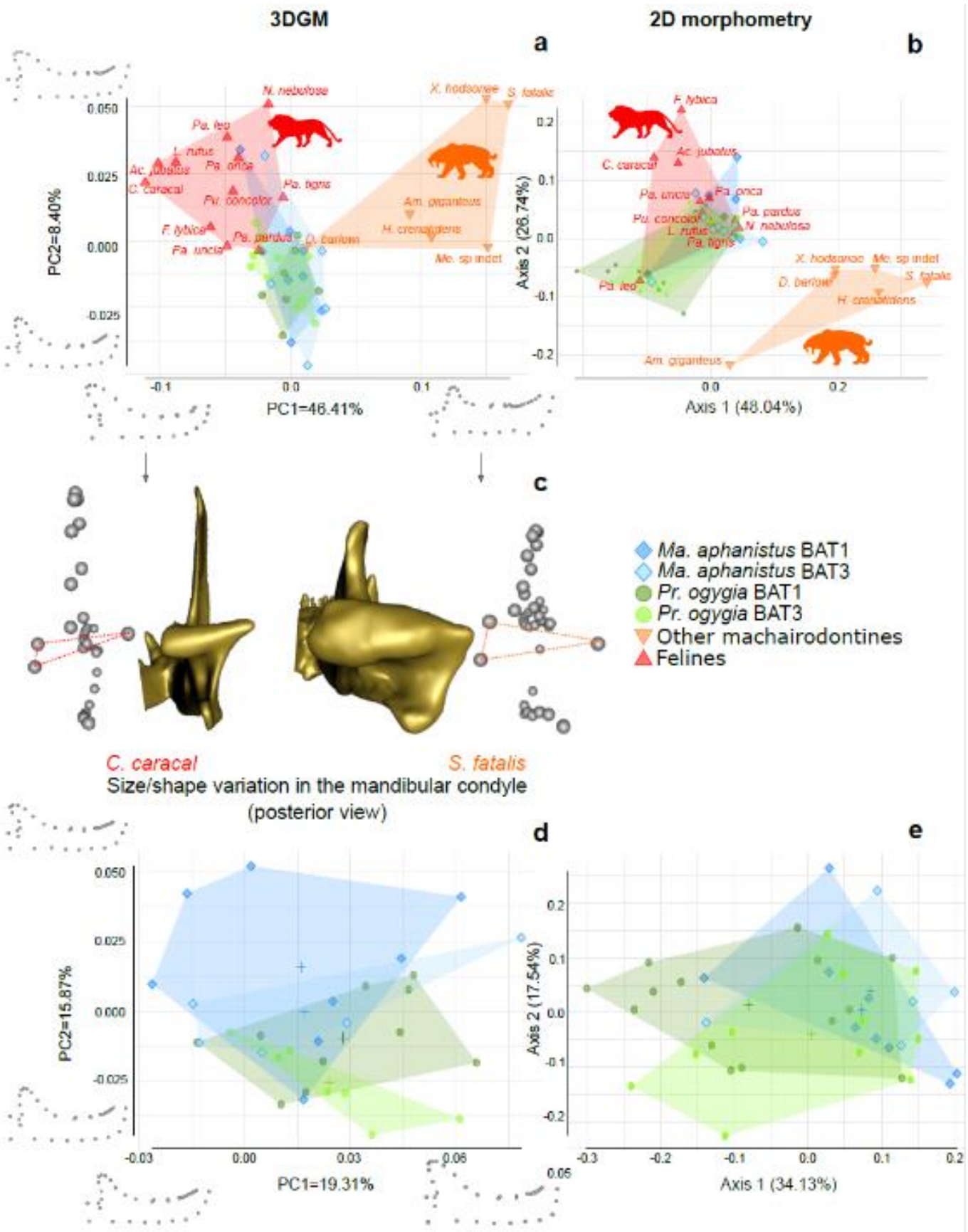
3DGM
2D morphometry
a
b
c
d
e
PC2=8.40%
PC1=46.41%
Axis 2 (26.74%)
Axis 1 (48.04%)
N. nebulosa
X. hodsoniae
S. fatalis
Pa. leo
L. rufus
Ac. jubatus
Pa. onca
C. caracal
Pa. tigris
Pu. concolor
Am. giganteus
H. crenatidens
F. lybica
Pa. pardus
D. barlowi
Pa. uncia
Me. sp indet
Ma. aphanistus BAT1
Ma. aphanistus BAT3
Pr. ogygia BAT1
Pr. ogygia BAT3
Other machairodontines
Felines
C. caracal
S. fatalis
Size/shape variation in the mandibular condyle
(posterior view)
PC2=15.87%
PC1=19.31%
Axis 2 (17.54%)
Axis 1 (34.13%)

Table 3: *Influences of each variables on the PcoA (on the whole sample) first two axes given by envfit function. Variables with a significant p-value for the regressions (under a 0.05 threshold) are marked in bold.*

	Axis 1	Axis 2	R^2	p-value
p3	**-0.98612**	**0.16602**	**0.3270**	**0.006**
Vestigial p3	**0.96916**	**-0.24642**	**0.4052**	**0.003**
p2	**-0.54807**	**-0.83643**	**0.8599**	**0.001**
CPc1L/ML	**-0.72341**	**0.69042**	**0.5880**	**0.001**
CTL/m1cL	**-0.80923**	**0.58749**	**0.8067**	**0.001**
(m1CL-DL-CTL)/m1CL	-0.93358	0.35837	0.1623	0.051
DL/(DL+CTL)	**0.70752**	**-0.70670**	**0.7328**	**0.001**
m1CL/ML	0.53474	0.84502	0.0283	0.576
APm1L/ML	**-0.37468**	**0.92716**	**0.5687**	**0.001**
APCPH /ML	**-0.31879**	**0.94783**	**0.4732**	**0.001**
APMCH/APCPH	**0.81145**	**-0.58443**	**0.2083**	**0.019**
DL/ML	**0.88290**	**0.46955**	**0.7814**	**0.001**
SH/ML	0.81359	0.58143	0.1231	0.103

Axis 2 values increase with the lack of p2, an increased distance between the lower canine and the m1 (m1cL/ML), a more developed posterior part of the mandible (from the notch of the m1 to the angular process, high APm1L/ML) and an increased height of the coronoid process (APCPH/ML). On this axis, felines occupy the highest values, and *Pr. ogygia* and *Ma. aphanistus* recover pretty well the feline space. In the first two axes of the PCoA, the sabertoothed felids from Batallones occupy a position more similar to that of extant felines than in the PCA based on 3D Procrustes coordinates. However, the relative position of the individual seemed similar and the mantel test corroborate this observation with a p-value of 0.001.

The cluster dendrogram recovers three main groups (see number on branches Fig. S2). With the exception of *Pr. ogygia*, *Ma. aphanistus*, and *Amphimachairodus giganteus*, sabertoothed felids form a clearly distinct

group from extant felines and are united in the first group. The first group is characterized by typical sabertooth features, such as the lack of p2, a high symphysis region or a long diastema, but also reduced cheek teeth length. Within this group, *Smilodon* and *Xenosmilus* are clustered by the lack of p2 and p3, but also some highly similar ratio such as for the symphysis height (respectively 0.334675311 and 0.337163814) or the height between the angular process and the mandibular condyle (0.398358256 and 0.394229829). *Dinofelis barlowi, Homotherium crenatidens,* and *Megantereon* share a vestigial p3 and lack the p2, and have ratios somewhat different from those of *S. fatalis* and *X. hodsonae*. The second and third group incorporates all specimens that notably have a short symphysis, a short diastema, and an increased length of check teeth. The second group comprising *Amphimachairodus*, *Panthera leo*, and machairodontines from Batallones mainly differs from the third by having a slightly longer symphysis, an increased length between the lower canine and the distal part of the m1, and a vestigial p2. The third and last group consist of the extant felines (without *Pa. leo*) and some specimens from Batallones lacking the p2. As was suspected by morphospace occupation, the cluster dendrogram suggests that *Pr. ogygia* and *Ma. aphanistus* are closer to felines than to the more derived machairodontines in their mandibular architecture.

Morphological differences between Batallones-1 and Batallones-3

We first performed a principal component analysis on 3D GM data restricted to the Batallones sample (Fig. 4d), in order to assess whether geographical and temporal differences are present. The PCA recovered 29 axes with the first two accounting for 35.19% of the variation (19.31% for PC1, 15.87% for PC2). Procrustes coordinates with the highest loadings on PC1 were (in a decreasing order) the ventral line of the mandible and symphysis region and the coronoid process, the other being close to 0. Increasingly positive values on PC1 correspond to a straighter symphyseal region, a straighter ventral plane of the dentary, and a larger mandibular condyle. Taxa with increasingly negative values of PC1 have longer diastema and straighter and shorter coronoid process, which are considered as derived machairodontine characters (Kurtén 1952; Emerson and Radinsky 1980; Martin 1980; Radinsky and Emerson 1982; Miller 1984; Akersten 1985; Turner and Antón 1997). Taxa with increasingly negative values of PC2 have a straighter symphyseal region, relatively shorter diastema, and a high and straight coronoid process, while positive values along the PC2 axis show a rostrally projected symphysis, a longer diastema, and a posteriorly projected coronoid process. Procrustes coordinates with the highest loadings on PC2 were (in a decreasing order) the coronoid process, the ventral line of the mandible, and symphysis region.

The morphospace restricted to the Batallones felids reveals a more important intraspecific variation for *Ma. aphanistus* than for *Pr. ogygia*, at least along the first two axes, even though the *Pr. ogygia* sample included four more individuals. Even if they do not overlap perfectly, the variation between sites appears minor. *Promegantereon ogygia* and *Ma. aphanistus* clearly overlap along the PC1, but PC2 better separates both taxa, as the latter occupies more positive values, while *Pr. ogygia* exhibits more negative ones. Without the context provided by the whole sample and, as so-called derived machairodontine features are scattered in negative and positive values on each axis, it is difficult to interpret one species as more derived than the other. Batallones-1 individuals occupy a wider area in the morphospace but there is also more specimens from that site.

We also tested this per-site difference by computing a principal coordinates analysis on the dataset containing the ratios and the discrete data (see Table S3**)**. This PCoA ordination recovered 17 axis with Axis 1 explaining 46.97% of variance and Axis 25.07%. As both *Pr. ogygia* and *Ma. aphanistus* have a well-developed and functional p3, the two characters describing this tooth became non-informative and were removed from the matrix. The characters influencing this analysis the most are: the presence/absence of a p2, the length of the cheek teeth compared to the length between the lower canine and the most distal point of m1 (CTL/m1cL), the mesiodistal length of the lower canine compared to the length between the lower canine and the most distal point of m1 ((m1cL-DL-CTL)/m1cL), the diastema length compared to the total length of the mandible (DL/ML), and the length between the lower canine and the most distal point of m1 (DL/m1cL) (see Table 2). Axis 1 values increase mainly when p2 disappears and when the coronoid process decreases in size (low APCPH/ML). Concerning Axis 2, positive values indicate a more posteriorly projected coronoid process (high CPC1L/ML), long cheek teeth length compared to the mandible size (high CTL/ML), a longer mesiodistal lower canine length (high (m1cL-DL-CTL)/m1cL), a reduced diastema length compared to the post canine teeth length (low DL/(DL+CTL)), a long proportion of the mandible occupied by the teeth and the diastema (high m1cL/ML), a more developed posterior part of the mandible (from the notch of the m1 to the angular process, high APm1L/ML), an increased height between the angular process and the mandibular condyle compared to the height of the mandible (high APMCH/APCPH), a longer diastema in comparison to the mandible length (high DL/ML), and a shorter symphysis (low SH/ML). *Promegantereon ogygia* occupy a region in PCoA with the lowest values on Axis 1 and Axis 2 (Fig. 4e) but that still clearly overlaps with *Ma. aphanistus*. This latter and *Pr. ogygia* overlap completely on the average values on Axis 2 (from -0.15 to 0.15). Also, seeing the results of the NMDS analysis (Fig. S3)

the original dissimilarities are well represented in two dimensions. In fact, as the distribution in the Shepard diagram appears to be remarkably linear the PCoA distances are almost identical to the original ones.

The Procrustes ANOVA indicates that there are no significant differences in terms of mandibular shape between the individuals from Batallones-1 and Batallones-3 (p-value = 0.44 for *P. ogygia* between Batallones-1 and Batallones-3, and p-value = 0.27 for *Ma. aphanistus*). These results converge with the observations based on the morphospaces occupation as the centroids are extremely close (see Fig. 4d, e or Table S5 for the exact centroids coordinates). Also, the PERMANOVA did not retrieve either any significant differences between Batallones-1 and Batallones-3 regarding the distance matrix based on the measurements and binary variables (p-value=0.1239 for *Pr. ogygia* and 0.1379 for *Ma. aphanistus*).

Intraspecific variation in the mandibular shape of late Miocene machairodontines

We studied the intraspecific variation of each Batallones machairodontine taxon, using the Procrustes coordinates and the linear/categorical dataset (Fig. S4a, b). While the total variation computed on the Procrustes 3D coordinates suggests a higher variation among the specimens of *Ma. aphanistus* from Batallones-3; such a difference is not found in the other dataset (Fig. S4b). *Promegantereon ogygia* is more common in Batallones (nine individuals from Batallones-1, and eight from Batallones-3 were complete enough to place landmarks) and its variation is similar in both sites using Procrustes coordinates and the dissimilarity matrix (Fig. S5). Even if the p-value is uncommonly low (down to 4.4e-10 for Fig. S5b), the boxplots of Batallones-1 and Batallones-3 show relatively similar distributions of bootstrapped disparity values; the difference between both sites is thus significant when 1000 bootstraps are computed, but remains very small.

Then, variation in mandibular shape of *Ma. aphanistus* and *Pr. ogygia* was compared using only the dissimilarity matrix stemming from linear measurements and categorical data to have more individuals. *Promeganteron ogygia* has a higher intraspecific variation than *Ma. aphanistus* in terms of mandibular measurements (Fig. S6) and this difference is significant (p−value=2.2e−53), with a disparity value ranging from 0.0038 to 0.0050 for *Ma. aphanistus* and from 0.0044 to 0.0058 for *Pr. ogygia*.

DISCUSSION

Morphospace occupation of early machairodontines

The evolutionary relationships within machairodontines are still unclear (Werdelin and Flinck 2018; Geraads and Spassov 2020). On one side, there are the few, recent phylogenetic analyses

(e.g., Christiansen 2013; Wallace and Hulbert 2013; Werdelin and Flinck 2018) and on the other side, the more 'traditional' tribe subdivisions based on phenetics (e.g., Kurtén 1952, 1968; Beaumont 1964, 1978; Martin 1980, 1998; Turner and Antón 1997; Werdelin et al. 2010; Antón 2013; Siliceo et al. 2014) that divides Machairodontinae into three groups: Smilodontini, Homotherini, and Metailurini. In this traditional point of view, Smilodontini comprises genera such as *Smilodon*, *Megantereon*, *Rhizosmilodon,* and *Promegantereon,* while Homotherini includes, among others, *Homotherium, Xenosmilus, Machairodus,* and *Amphimachairodus;* finally Metailurini consists mainly of *Adelphailurus*, *Dinofelis,* and *Metailurus* (Kurtén 1952, 1968; Beaumont 1964, 1978; Martin 1980, 1998; Turner and Antón 1997; Sardella 1998; Antón and Galobart 1999; Martin et al. 2000; Werdelin et al. 2010; Rincón et al. 2011), although this tribe is sometimes considered as a wastebasket group (Werdelin et al. 2010). In our mandibular morphospace analyses, the individuals belonging to the same 'tribe' often do not cluster together. This traditional, phenetic subdivision was mainly based on upper canine morphology (e.g., dirk vs. scimitar shape, serrated or not) (Kurtén 1952, 1965; Beaumont 1964, 1978; Martin 1980, 1998; Berta and Galiano 1983; Turner and Antón 1997; Antón and Galobart 1999; Antón et al. 2004; Slater and Van Valkenburgh 2009), which were not included in our analysis. The presence of possible anagenetic lineages (Smilodontini and Homotherini) is still a controversial subject (Geraads and Spassov 2020) but it seems that mandibular shape does not support this hypothesis. With the mandible being almost entirely devoted to mastication, it is closely linked to feeding habits among Carnivora (Raia 2004; Meloro 2011; Meloro and O'Higgins 2011; Meloro et al. 2011, 2015; Prevosti et al. 2012) and it is thus not surprising to be highly similar in taxa with supposedly comparable hunting methods like 'Smilodontini' and 'Homotherini', even if Figueirido et al. (2018) suggested they may have distinct predatory behaviour based on FEA analyses. Mandibular morphology also informs another taxonomic debate, regarding the distinctness of *Ma. aphanistus* and *Am. giganteus*. Indeed, there are two hypotheses concerning these species: they are either regarded as belonging to two distinct genera (*Machairodus* and *Amphimachairodus,* e.g., Turner et al. 2011; Salesa et al. 2012; Christiansen 2013; Monescillo et al. 2014; Werdelin and Flinck 2018; Antón et al. 2013, 2020) or as belonging to two species representing earlier and later stages of evolution of the same genus (e.g., Geraads and Spassov 2020). This debate is still open and quite difficult to disentangle due to the presence of mosaic evolution but all authors agree on the presence of a lineage from *Ma*. *aphanistus* to *Am. giganteus* and the controversy is focused on whether or not a genus name can change within an anagenetic lineage. In our analyses, the mandibular shape of *Am. giganteus* appears clearly dissimilar, being much more derived than that of *Ma.*

aphanistus, However, our analysis is only based on the mandible, so that further morphometric comparative studies on other morphological structures should be performed to refine the taxonomic status of those species.

Also, our linear regressions did not retrieve a clear correlation between mandible size and position within the morphospace (Table S4 and Fig. S1). Some authors found significant relations between body size/prey size and mandible size such as a lengthening of the dentary in felids that take large prey to produce greater gapes (Slater and Van Valkenburgh 2009) or a lengthening of the distance between the jaw joint to the canine (Christiansen and Adolfssen 2005). However, when studied as a whole the mandible appears to be shaped by other factors than just skull size.

Our three-dimensional landmarks analysis provides new clues about the variation of the mandibular condyle morphology. The morphology of the condyle is rarely discussed in the literature, and only early monographs, such as that by Ballésio (1963), highlighted the importance of its size; most authors just dealt with its position (more ventrally or dorsally located) (Bonis 1975; Beaumont 1975; Werdelin and Lewis 2000; Christiansen 2012; Antón et al. 2014). As the dentary is almost always photographed or drawn in a lateral view, the anatomy of the condyle in posterior view is poorly known. In felines and machairodontines, the condyle has a triangular shape, being thinner on its lateral side, and becoming thicker medially. However, it is oriented laterally in felines and medially in machairodontines. The most striking trait is the size, with the condyle being much larger among machairodontines (Fig. 4c, 5). On the contrary, the position of this condyle (more ventrally or dorsally located), which is more frequently discussed in the literature, does not vary much within our dataset. With machairodontines having the ability to open the mouth at incredibly large gapes (Akersten 1985), a larger mandibular condyle could confer a stronger support for the mandible when the mouth is wide open. A few studies have investigated the biomechanical properties of the mandibles or skulls of sabertooth felids (McHenry et al. 2007; Figueirido et al. 2018; Lautenschlager et al. 2020). However, the biomechanical role played by the mandibular condyle has not yet been investigated, and our study suggests that it should be taken into account in future studies. Our study also emphasizes that 2D geometric morphometrics that rely on lateral views (e.g., Christiansen 2008a, 2008b, 2012; Slater and Van Valkenburgh 2009; Prevosti et al. 2010; Christiansen and Harris 2012; Stubbs et al. 2013; Piras et al. 2013; Navarro et al. 2018; Schaeffer et al. 2019) might miss potentially important features and variation.

Extant felines display a conservative mandibular morphology, resembling that of the earliest felids, while machairodontines clearly expanded the ancestral felid bauplan. Cranial,

dental, and mandibular characters linked to the sabertooth morphology have already been abundantly described (Kurtén 1952; Emerson and Radinsky 1980; Martin 1980; Radinsky and Emerson 1982; Miller 1984, Akersten 1985; Turner and Antón 1997). As early sabertoothed felids, *Pr. ogygia* and *Ma. aphanistus* retain some morphological traits with feline/primitive felids, but also show some of these derived sabertooth characters. Indeed, both species almost lost the p2, although some individuals still present a vestigial one (Fig. 6a, b, d). In our sample, a vestigial p2 or alveolus for p2 was observed in about half of the *Pr. ogygia* individuals (9/16 from Batallones-1 and 4/9 from Batallones-3) (Fig. 6a-c) but was less common in *Ma. aphanistus,* with only two out of ten individuals from Batallones-1 and two out of seven from Batallones-3. In fact, only one specimen of *Ma. aphanistus* shows an alveolus indicating the presence of a p2 (BAT-3'13 1916b, Fig. 6d), while the others only have the alveolus that seems to have been reabsorbed during the mandible growth (Fig. 6e). Salesa et al. (2012b) observed a similar alveolus when describing of the p2 of *Leptofelis vallesiensis*, a small feline also present in Batallones-1 and Batallones-3. They suggested that the tooth observed was not a p2, but a retained dp2 that was never replaced by the p2. This could be the case for *Ma. aphanistus* as well, pending a detailed analysis of the alveolar bone histology of this taxon. *Promegantereon ogygia* always develops a p2 or at least a complete alveolus in the individuals where this feature could be assessed (n=15), and it can be assumed that the tooth observed in *Pr. ogygia* is an actual p2 (Salesa et al. 2010a). Also, *Ma. aphanistus* shows a more developed talonid on the m1, a deeper notch between the protoconid and the paraconid, and a more developed mesial cuspid on the p3 (Fig. 7). *Machairodus aphanistus* also has relatively large lower canines, but the incisors are small, forming a straight dental row with the canines (Ginsburg et al. 1981; Antón et al. 2004). Nevertheless, the canines and the incisors of *Ma. aphanistus* form a slightly curved row compared to the straight dental row seen in *Pr. ogygia*. Both species present a symphyseal region that is straighter than those of felines (Antón et al. 2004; Salesa et al. 2005) but not as straight as in more recent, derived machairodontines. Thus, *Pr. ogygia* verges slightly closer to the saber-tooth morphology than *Ma. aphanistus* based on lower cheek tooth morphology and dimensions. Both *Pr. ogygia* and *Ma. aphanistus* show elongated and laterally flattened upper canines, and a relatively straightened mandibular symphysis (Antón et al. 2004; Salesa et al. 2005). However, contrary to *Pr. ogygia,* the upper canines *of Ma. aphanistus* are crenulated, like those of other derived machairodontines such as *Homotherium* (Antón et al. 2004). The symphysis of *Pr. ogygia* is straighter than that of *Ma. aphanistus*; as a result, *Pr. ogygia* and *Ma. aphanistus* exhibit different combinations of the so-called ‘sabre-tooth adaptations’ (Antón et al. 2004; Salesa et al. 2005), which is in accordance with our morphospace

analyses, where these taxa lie in-between extant felines and more derived machairodontines. (Fig. 4a, b). These results are in line with other previous studies such as those of Christiansen (2006, 2008*a*, 2008b), Christiansen and Harris (2012), Prevosti et al. (2010), or Piras et al. (2013, 2018). However, Batallones taxa seem somewhat closer to the felines than to their sabertoothed counterparts, which could indicate different ecomorphologies among Machairodontinae as suggested by Werdelin and Lewis (2000). Also, *Pr. ogygia* and *Ma. aphanistus* present different degrees of sabertoothed adaptations in their own ways. *Promegantereon ogygia* and *Ma. aphanistus* each exhibit a distinct mosaic of primitive and derived features, confirming previous studies (Antón et al. 2004; Salesa et al. 2005). Adding more primitive felids and machairodontines (i.e., *Pseudaelurus*) and 'Metailurini' (i.e., *Metailurus*) will be necessary to assess whether there is a continuum between the 'feline space' and the machairodontine one.

Promegantereon ogygia seems to occupy a larger morphospace on the PCoA than *Ma. Aphanistus,* which suggests, in our case, a greater variability, confirmed by our bootstrapping procedure (Fig. S5). Our PCA shows that early machairodontines morphological space (corresponding to low PC2 and average PC1 values) is characterized by a relatively high but straight coronoid process. The coronoid process projects posteriorly in felines, and is straight and short in derived machairodontines (Fig. 5). Although less conspicuous, a comparable situation is found in the PCoA, where early machairodontines (most especially *Pr. ogygia*) explore a region within the negative values of the Axes 1 and 2, where only the extant *Pa. leo* is located.

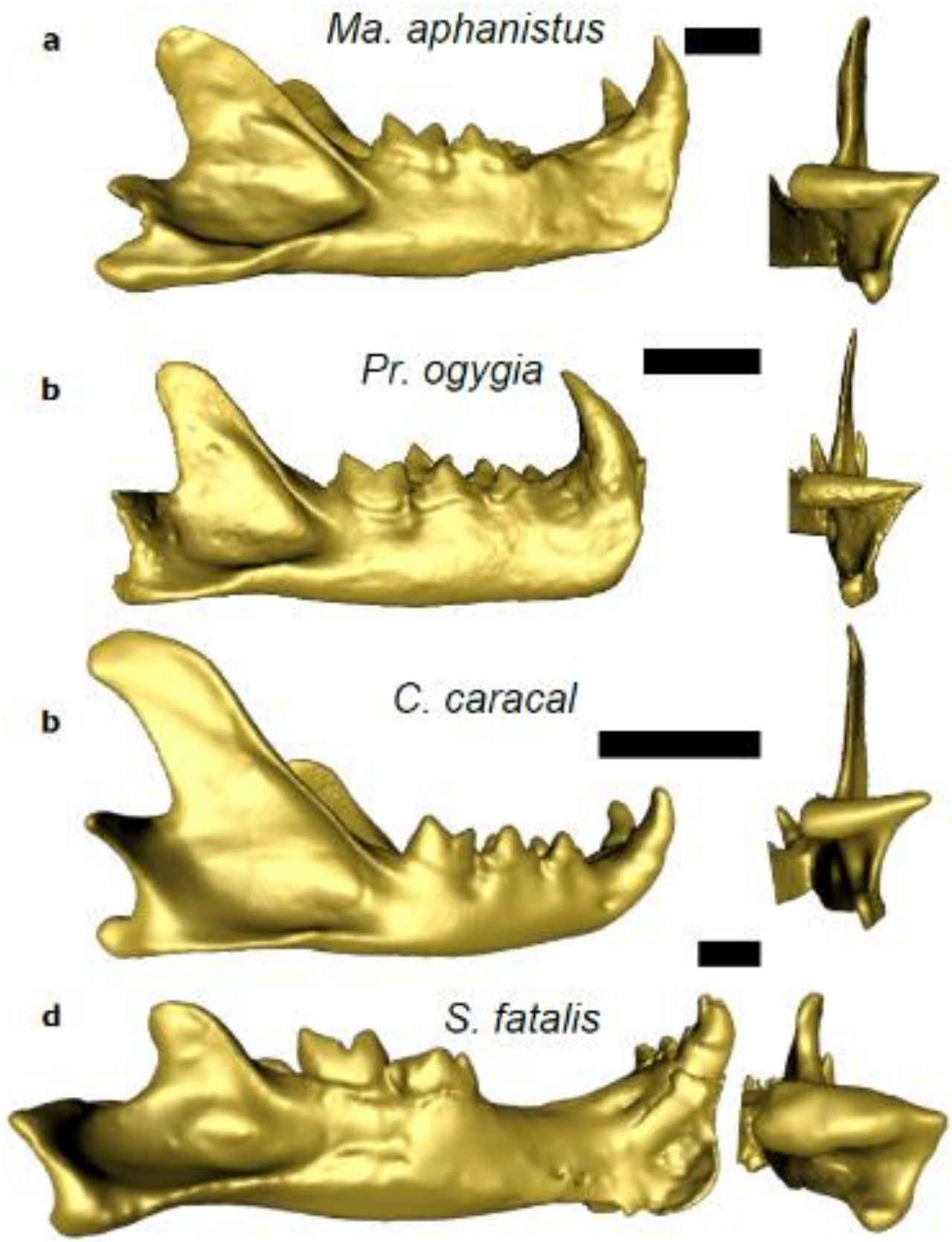

***Figure 5**: Lateral (left) and posterior (right) views of the mandibles of Ma. aphanistus (BAT-3'09 1344; a), Pr. ogygia (BAT-3'10 1773; b), C. caracal (MAV-1518; c), and S. fatalis (M7786-9732; d) for comparisons of the morphology of the coronoid process (left) and mandibular condyle (right) posterior.*

As mentioned above, most of the individuals found in Batallones are young adults except for two specimens of *Pr. ogygia* (B-7042 and B-5198), which have worn teeth, as did all the derived machairodontines and felines in our dataset. This age difference between some specimens of *Pr. ogygia* and *Ma. aphanistus,* and the rest of the dataset could introduce shape variations of the mandible. For instance, our analysis demonstrated a great variability in the shape of the coronoid process among *Pr. ogygia* and *Ma. aphanistus,* with morphologies that were not observed in other analyzed felids. Ontogeny of the felid mandible has been already studied showing that the shape of the coronoid process undergoes substantial changes during the lifespan of an individual, as shown by Segura (2015) for *Lynx rufus,* or by Biknevicius and Leigh (1997) and Giannini et al. (2010) for *Puma concolor*. These changes consist in a global enlargement of the coronoid process (Biknevicius and Leigh 1997; Segura 2015), which is more dorsally projected among adults and more posteriorly projected in juvenile individuals (Giannini et al. 2010). Segura (2015) explained these changes by a growing influence of the m. temporalis and m. masseter approaching adulthood. Nevertheless, according to these authors, all these changes occurred before adulthood, and thus, they could not explain the variation observed as all the specimens from the dataset have their adult dentition. Therefore, the variations in coronoid shape we observe in our sample cannot be explained by differences in ontogenetic stages.

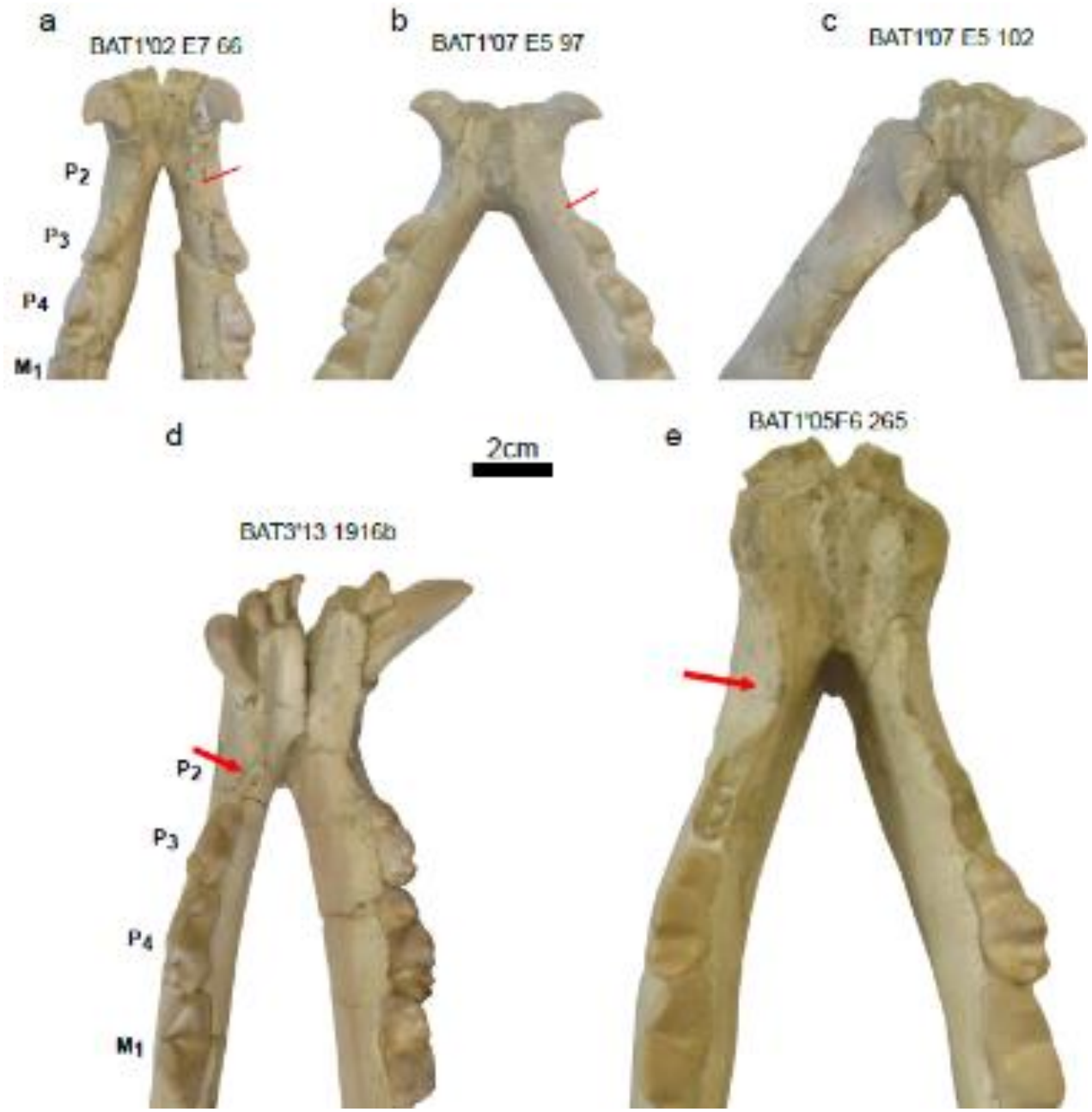

***Figure 6**: Variability in the presence of a p2 in Pr. ogygia (a, b, c) and Ma. aphanistus (d, e). a: BAT1'02 E7 66; b: BAT1'07 E5 97; c: BAT1'07 E5 102, d: BAT-3'13 1916b; e: BAT-1'05 F6 265. The red arrow indicates the presence of a p2 (a) or just an alveolus (b, d, e; bone regrowth present in e). The alveolus is not even present in c.*

Intraspecific variation between sites

Our analyses converge in rejecting the hypothesis of a significant variation of mandibular morphology of each machairodontine species (*Pr. ogygia* and *Ma. aphanistus*) between Batallones-1 and 3. In addition, *Pr. ogygia* and *Ma. aphanistus* have a clearly overlapping morphospace occupation. Thus, it is clear that the populations from Batallones-1 and Batallones-3 are quite homogenous

regarding mandibular shape. Our results thus diverge from those of Siliceo et al. (2014) and Monescillo et al. (2014) who found significant differences in dental morphology and talocalcaneal anatomy between the populations of both sites. Although we studied the same taxa, our results rely on different analyses (Procrustes ANOVA, PERMANOVA, PCA, PCoA, clustering) whereas the results obtained in 2014 are based on a smaller sample and single test (Student's t-test)**.** Nevertheless, our results and those from Siliceo et al. (2014) and Monescillo et al. (2014) show the mosaic nature of the sabertoothed felids, and how different body parts were evolving at a different rate.

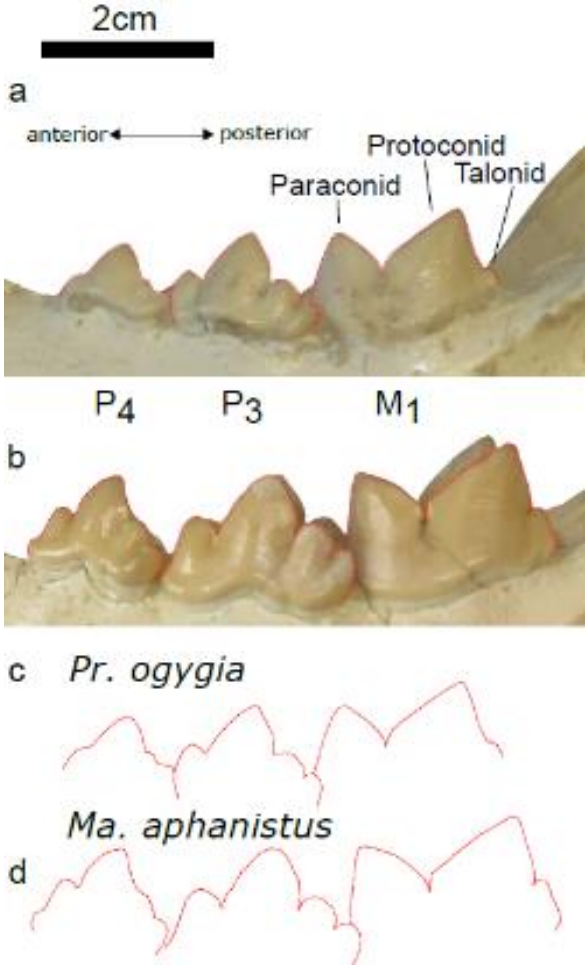

Comparison of signals from 3D GM and linear measurements

Both the linear and 3D GM datasets are partially independent (encompassing different yet overlapping anatomical regions) and their treatment is also distinct, as the notion of space or geometry is evidently absent in the 'linear' dataset. Few studies confronted these two methods on the same dataset to study vertebrates (Bernal 2007; Jedensjö et al. 2020), but overall geometric morphometric was far more powerful than linear morphometry. While three-dimensional geometric morphometrics and linear measurements produced two different morphospaces, the position of each 'group' relative to one another does not vary so much as confirmed by the Mantel test. In both analyses, felines and machairodontines are clearly separated. Also, *Pr. ogygia* and *Ma. aphanistus* always occupy a position in between felines and machairodontines, but are somewhat closer to felines in the morphospace of linear measurements. In both morphospaces, small felines and derived machairodontines are the most distant taxa and thus exhibit the greatest differences in mandible shape. In extant felines, there is a clear morphological threshold between small species hunting prey much smaller than themselves to larger species hunting prey up to 45% larger than themselves (Carbone et al. 1999, 2007).

Figure 7*: Comparison of the dental outline of Pr. ogygia (BAT1'07 E5 97) and Ma. aphanistus (BAT3'13 1916b) in lateral view (a, b) and schematic drawing (c, d).*

There is a considerable difference within felids between the derived machairodontines hunting method (canine shear bite) and that of felines (Turner and Antón 1997) which probably explains this clear gap between small bodied felines and the most recent machairodontines. This also agrees with some of the results obtained by Lautenschlager et al. (2020), where derived machairodontine taxa occupy morphospace regions associated with higher performance compared to basal forms for certain biomechanical parameters such as maximum jaw gape or bending strength.

CONCLUSIONS

The abundant and well-preserved fossils of the sabertoothed felids *Pr. ogygia* and *Ma. aphanistus* from Batallones-1 and Batallones-3 sites offer a unique opportunity to analyse population disparity in early machairodontine felids. While further comparative studies are required to fully understand the functional differences between primitive and derived sabertoothed machairodontines, *Pr. ogygia* and *Ma. aphanistus* occupy a position in the mandibular morphospaces that lies closer to felines than to derived machairodontines. The overall mandible shape when studied with 3D GM is not influenced by allometry. Concerning the mandible morphology, our analyses reject the hypothesis of a morphological shift between these two localities. Our analyses also reveal that both the size and orientation of the mandibular condyle is peculiar in machairodontines, their condyles are large and lingually oriented while the condyles of felines are smaller and buccally oriented. This suggest strong differences in the biomechanics of the bite between both groups.

REFERENCES

Adams DC, Otárola-Castillo, E (2013) geomorph: an R package for the collection and analysis of geometric morphometric shape data. Methods Ecol Evol 4(4):393–399

Adams JW, Olah A, McCurry MR, Potze S (2015) Surface model and tomographic archive of fossil primate and other mammal holotype and paratype specimens of the Ditsong National Museum of Natural History, Pretoria, South Africa. PLoS One 10(10): e0139800. doi:10.1371/journal.pone.0139800

Akersten WA (1985) Canine function in *Smilodon* (Mammalia: Felidae: Machairodontinae). Sci Nat Hist Mus Los Angeles County 356:1–22

Anderson MJ (2001) A new method for non-parametric multivariate analysis of variance. Austral Ecol 26(1):32–46

Antón M, Galobart À (1999) Neck function and predatory behavior in the scimitar toothed cat *Homotherium latidens* (Owen). J Vertebr Paleontol 19(4):771–784

Antón M, Salesa MJ, Galobart A, Tseng ZJ (2014) The Plio-Pleistocene scimitar-toothed felid genus *Homotherium* Fabrini, 1890 (Machairodontinae, Homotherini): diversity, palaeogeography and taxonomic implications. Quat Sci Rev 96:259-268. doi:10.1016/j.quascirev.2013.11.022

Antón M, Salesa MJ, Morales J, Turner A (2004) First known complete skulls of the scimitar-toothed cat *Machairodus aphanistus* (Felidae, Carnivora) from the Spanish late Miocene site of Batallones-1. J Vertebr Paleontol 24(4):957-969. doi: 10.1671/0272-4634(2004)024[0957:FKCSOT]2.0.CO;2

Antón M, Salesa MJ, Siliceo G (2013) Machairodont adaptations and affinities of the Holarctic late Miocene homotherin *Machairodus* (Mammalia, Carnivora, Felidae): the case of *Machairodus catocopis* Cope, 1887. J Vertebr Paleontol 35(3):1202-1213. doi:10.1080/02724634.2013.760468

Antón M, Siliceo G, Pastor JF, Morales J, Salesa MJ (2020) The early evolution of the sabertoothed felid killing bite: the significance of the cervical morphology of *Machairodus*

aphanistus (Carnivora: Felidae: Machairodontinae). Zool J Linnean Soc 188(1):319-342. doi:10.1093/zoolinnean/zlz086

Antón M (2013) Sabertooth. Indiana University Press, Bloomington

Ballésio R (1963) Monographie d'un "*Machairodus*" du gisement villafranchien de Sénèze: *Homotherium crenatidens* Fabrini. Le Hénaffe, Saint Etienne

Bernal V (2007) Size and shape analysis of human molars: comparing traditional and geometric morphometric techniques. Homo 58(4):279–296

Berta A, Galliano H. (1983) *Megantereon hesperus* from the late Hemphillian of Florida with remarks on the phylogenetic relationships of machairodonts (Mammalia, Felidae, Machairodontinae). J Paleontol 57:892–899

Biknevicius AR, Leigh SR (1997) Patterns of growth of the mandibular corpus in spotted hyenas (*Crocuta crocuta*) and cougars (*Puma concolor*). Zool J Linnean Soc 120(2):139–161

Bookstein FL (1997) Morphometric Tools for Landmark Data: Geometry and Biology. Cambridge University Press, Cambridge

Butler RJ, Brusatte SL, Andres B, Benson RB (2012) How do geological sampling biases affect studies of morphological evolution in deep time? A case study of pterosaur (Reptilia: Archosauria) disparity. Evolution 66(1):147-162. doi:10.1111/j.1558-5646.2011.01415.x

Calvo JP, Pozo M, Silva PG, Morales J (2013) Pattern of sedimentary infilling of fossil mammal traps formed in pseudokarst at Cerro de los Batallones, Madrid Basin, central Spain. Sedimentology 60:1681-1708. doi:10.1111/sed.12048

Carbone C, Mace GM, Roberts SC, Macdonald DW (1999) Energetic constraints on the diet of terrestrial carnivores. Nature 402:286–288

Carbone C, Teacher A, Rowcliffe JM (2007) The costs of carnivory. PLoS Biol 5(2) e22. doi: 10.1371/journal.pbio.0050022

Christiansen P (2006) Sabertooth characters in the clouded leopard (*Neofelis nebulosa* Griffiths 1821). J Morphol 267(10):1186-1198. doi:10.1002/jmor.10468

Christiansen P (2008a) Evolution of skull and mandible shape in cats (Carnivora: Felidae). PLoS One 3(7): e2807. doi:10.1371/journal.pone.0002807

Christiansen P (2008b) Evolutionary convergence of primitive sabertooth craniomandibular morphology: the clouded leopard (*Neofelis nebulosa*) and *Paramachairodus ogygia* compared. J Mammal Evol 15:155-179. doi:10.1007/s10914-007-9069-z

Christiansen P (2012) The making of a monster: Postnatal ontogenetic changes in craniomandibular shape in the great sabercat Smilodon. PLoS One 7(1): e29699. doi: 10.1371/journal.pone.0029699

Christiansen P (2013) Phylogeny of the sabertoothed felids (Carnivora: Felidae: Machairodontinae). Cladistics 29(5):543-559. doi:10.1111/cla.12008

Christiansen P, Adolfssen J (2005) Bite forces, canine strength and skull allometry in carnivores (Mammalia, Carnivora). J Zool 266(2):133-151. doi:10.1017/S0952836905006643

Christiansen P, Harris JM (2012). Variation in craniomandibular morphology and sexual dimorphism in pantherines and the sabercat *Smilodon fatalis*. PLoS One 7(10):e48352. 10.1371/journal.pone.0048352

Cignoni P, Callieri M, Corsini M, Dellepiane M, Ganovelli F, Ranzuglia G (2008) Meshlab: an open-source mesh processing tool. Eurographics Italian chapter conference 2008:129–136

Cooke HBS (1991) *Dinofelis barlowi* (Mammalia, Carnivora, Felidae) cranial material from Bolt's Farm collected by the University of California African expedition. Palaeontol Afric *28*:9–21

Beaumont G (1964) Remarques sur la classification des Felidae. Eclogae Geol Helvetiae 57(2):837–845

Beaumont G (1975) Recherches sur les félidés (mammifères, carnivores) du pliocène inferieur des sables à *Dinotherium* des environs d'Eppelsheim (rheinhessen). Archives des sciences 28(3):369–405

Beaumont G (1978) Notes complémentaires sur quelques Félidés (Carnivores). Archives des Sciences Physiques et Naturelles Genève 31(3):219–227

Bonis L (1975) Aperçu sur les Félinés Machairodontinés. Problèmes Actuels de Paléontologie-Évolution des Vertébrés 2:156–174

Dixon P (2003) VEGAN, a package of R functions for community ecology. J Veg Sci 14(6):927–930

Eisenberg JF (1981) The Mammalian Radiations: An Analysis of Trends in Evolution, Adaptation, and Behavior. University of Chicago Press, Chicago

Emerson SB, Radinsky L (1980) Functional analysis of sabertooth cranial morphology. Paleobiology 6(3):295–312

Figueirido B, Lautenschlager S, Pérez-Ramos A, Van Valkenburgh B (2018) Distinct predatory behaviors in scimitar-and dirk-toothed sabertooth cats. Curr Biol 28(20):3260-3266

Geraads D, Spassov N (2020) A skull of *Machairodus* Kaup, 1833 (Felidae, Mammalia) from the late Miocene of Hadjidimovo (Bulgaria), and its place in the evolution of the genus. Geodiversitas 42:123–137

Giannini NP, Segura V, Giannini MI, Flores D (2010) A quantitative approach to the cranial ontogeny of the puma. Mammal Biol 75(6):547–554

Gilleland E, Katz RW (2016) extRemes 2.0: an extreme value analysis package in R. J Stat Softw 72(8):1-39. doi:10.18637/jss.v072.i08

Ginsburg L, Morales J, Soria D (1981) Nuevos datos sobre los carnivoros de Los Valles de Fuentiduena (Segovia). Estud geol 37(5):383–415

Gower JC (1971) A general coefficient of similarity and some of its properties. Biometrics 27(4):857–871

Guillerme T (2018) dispRity: a modular R package for measuring disparity. Methods Ecol Evol 9(7):1755–1763

Jedensjö M, Kemper CM, Milella M, Willems EP & Krützen M (2020) Taxonomy and distribution of bottlenose dolphins (Genus tursiops) in australian waters: An osteological clarification. Canadian J Zool 98:461–479

Klingenberg CP (1996) Multivariate allometry. In: Marcus LF, Corti LF, Loy A, Naylor GJP, Slice DE (eds) Advances in Morphometrics. Springer, Boston, pp 23-49

Klingenberg CP (2016) Size, shape, and form: concepts of allometry in geometric morphometrics. Dev Genes Evol 226(3):113-137

Kurtén B (1952) The Chinese *Hipparion* fauna: a quantitative survey with comments on the ecology of the machairodonts and hyaenids and the taxonomy of the gazelles. Comment Biol 13:1–82

Kurtén B (1965) The Pleistocene Felidae of Florida. Bull Florida State Mus 9(6):215–273

Kurtén B (1968) Pleistocene Mammals of Europe. Weidenfeld & Nicolson, London

López-Antoñanzas R, Peláez-Campomanes P, Álvarez-Sierra MÁ, Garcia-Paredes I (2010) New species of *Hispanomys* (Rodentia, Cricetodontinae) from the upper Miocene of Batallones (Madrid, Spain). Zool J Linnean Soc 160(4):725-747. doi:10.1111/j.1096-3642.2010.00618.x

McHenry CR, Wroe S, Clausen PD, Moreno K, Cunningham E (2007) Supermodeled sabercat, predatory behavior in *Smilodon fatalis* revealed by high-resolution 3D computer simulation. Proc Natl Acad Sci USA 104(41):16010–16015

Meachen JA, O'Keefe FR, Sadleir RW (2014) Evolution in the sabre-tooth cat, *Smilodon fatalis*, in response to Pleistocene climate change. J Evol Biol 27(4):714-723. doi:10.1111/jeb.12340

Maechler M, Rousseeuw P, Struyf A, Hubert M, Hornik K (2011) Package 'cluster'. R package version 1 (2):56

Martin LD (1980) Functional morphology and the evolution of cats. Trans Nebr Acad Sci Affil Soc 8:141–154

Martin LD (1998) Felidae. In: Janis CM, Scott KM, Jacobs LL (eds) Evolution of Tertiary Mammals of North America, Volume 1. Terrestrial Carnivores, Ungulates, and Ungulate like Mammals. Cambridge University Press, Cambridge, pp 236–242

Martin LD, Babiarz JP, Naples VL. Hearst J (2000) Three ways to be a saber-toothed cat. Naturwissenschaften 87(1):41–44

Meloro C (2011) Feeding habits of Plio-Pleistocene large carnivores as revealed by the mandibular geometry. J Vertebr Paleontol 31(2):428–446

Meloro C, Clauss M, Raia P (2015) Ecomorphology of Carnivora challenges convergent evolution. Org Divers Evol 15:711–720. doi:10.1007/s13127-015-0227-5

Meloro C, O'Higgins P (2011) Ecological adaptations of mandibular form in fissiped Carnivora. J Mammal Evol 18(3):185–200

Meloro C, Raia P, Carotenuto F, Cobb SN (2011) Phylogenetic signal, function and integration in the subunits of the carnivoran mandible. Evol Biol 38:465–475. doi:10.1007/s11692-011-9135-6

Monescillo MF, Salesa MJ, Antón M, Siliceo G, Morales J (2014) *Machairodus aphanistus* (Felidae, Machairodontinae, Homotherini) from the late Miocene (Vallesian, MN 10) site of Batallones-3 (Torrejon de Velasco, Madrid, Spain). J Vertebr Paleontol 34(3), 699-709. doi:10.1080/02724634.2013.804415

Miller GJ (1984) On the jaw mechanism of *Smilodon californicus* Bovard and some other carnivores. Imperial Valley College Museum Occasional paper 7:1–107

Morales J, Capitán J, Calvo JP, Cesé C (1992) Nuevo yacimiento de vertebrados del Mioceno Superior al Sur de Madrid (Cerro Batallones, Torrejón de Velasco). Geogaceta 12:77–80

Morales J, Nieto M, Amezua L, Fraile S, Gómez E, Herráez E, Peláez-Campomanes P, Salesa MJ, Sánchez IM, Soria D (eds) (2000) Patrimonio Paleontológico de la Comunidad de Madrid, Volume 6. Consejería de Cultura, Madrid

Morales J, Pozo M, Silva PG, Domingo MS, López-Antoñanzas R, Álvarez Sierra MÁ, Antón M, Martín Escorza C, Quiralte V, Salesa MJ, Sánchez IM, Azanza B, Calvo JP, Carrasco P, García-Paredes I, Knoll F, Hernández Fernández M, van den Hoek Ostende L, Merino L, ven der Meulen AJ, Montoya P, Peigné S, Peláez-Campomanes P, Sánchez-Marco A, Turner A, Abella J, Alcalde GM, Andrés M, DeMiguel D, Cantalapiedra JL, Fraile S, García Yelo BA, Gómez Cano AR, López Guerrero P, Oliver Pérez A, Siliceo G (2008). El sistema de yacimientos de mamíferos miocenos del Cerro de los Batallones, Cuenca de Madrid: estado actual y perspectivas. Palaeontologica Nova 8:41–117

Navarro CA, Martin-Silverstone E, Stubbs TL (2018) Morphometric assessment of pterosaur jaw disparity. R Soc Open Sci 5:172130. doi:10.1098/rsos.172130

Palmqvist P, Torregrosa V, Pérez-Claros JA, Martínez-Navarro B, Turner A (2007) A re-evaluation of the diversity of *Megantereon* (Mammalia, Carnivora, Machairodontinae) and the problem of species identification in extinct carnivores. J Vertebr Paleontol 27(1):160-175. doi: 10.1671/0272-4634(2007)27[160:AROTDO]2.0.CO;2

Paradis E, Claude J, Strimmer K (2004) APE: analyses of phylogenetics and evolution in R language. Bioinformatics 20(2):289-290. doi:10.1093/bioinformatics/btg412

Piras P, Maiorino L, Teresi L, Meloro C, Lucci F, Kotsakis T, Raia P (2013) Bite of the cats: relationships between functional integration and mechanical performance as revealed by mandible geometry. Syst Biol 62(6): 878–900. doi:10.1093/sysbio/syt053

Piras P, Silvestro D, Carotenuto F, Castiglione S, Kotsakis A, Maiorino L, Melchionna M, Mondanaro A, Sansalone G, Serio C, Anna Vero V, Raia P (2018) Evolution of the sabertooth mandible: a deadly ecomorphological specialization. Palaeogeogr Palaeoclimatol Palaeoecol 496(1):166-174. doi:10.1016/j.palaeo.2018.01.034

Polly PD (2013) Geometric morphometric: analytical paleontology short course, Macquarie University. Indiana University. http://www.indiana.edu/~g562/PBDB2013/. Accessed 12 April 2019.

Prevosti FJ, Turazzini GF, Amelia Chemisquy M (2010) Morfología craneana en tigres dientes de sable: alometría, función y filogenia. Ameghiniana 47(2):239-256. doi:10.5710/AMGH.v47i2.9

Prevosti FJ, Turazzini GF, Ercoli MD, Hingst-Zaher E (2012) Mandible shape in marsupial and placental carnivorous mammals: a morphological comparative study using geometric morphometrics. Zool J Linnean Soc 164(4):836-855. doi: 10.1111/j.1096-3642.2011.00785.x

R Foundation for Statistical Computing. (2019). R: a language and environment for statistical computing, R Foundation, Vienna.

Radinsky L, Emerson S (1982) The late, great sabertooths. Nat Hist 91(4):50–57

Raia P (2004) Morphological correlates of tough food consumption in large land carnivores. Ital J Zool 71(1):45–50

Rincón AD, Prevosti FJ, Parra GE (2011) New saber-toothed cat records (Felidae: Machairodontinae) for the Pleistocene of Venezuela, and the Great American Biotic Interchange. J Vertebr Paleontol 31:468–478

Rohlf FJ, Slice D (1990) Extensions of the Procrustes method for the optimal superimposition of landmarks. Syst Biol 39(1):40–59

Salesa MJ, Antón M, Morales J, Peigné S (2012b) Systematics and phylogeny of the small felines (Carnivora, Felidae) from the late Miocene of Europe: a new species of Felinae from the Vallesian of Batallones (MN 10, Madrid, Spain). J Syst Palaeontol 10(1)87-102. doi: 10.1080/14772019.2011.566584

Salesa MJ, Antón M, Turner A, Morales J (2005) Aspects of the functional morphology in the cranial and cervical skeleton of the sabertoothed cat *Paramachairodus ogygia* (Kaup, 1832) (Felidae, Machairodontinae) from the late Miocene of Spain: implications for the origins of the machairodontine killing bite. Zool J Linnean Soc 144:363-377. doi:10.1111/j.1096-3642.2005.00174.x

Salesa MJ, Antón M, Turner A, Morales J (2006) Inferred behaviour and ecology of the primitive sabertoothed cat *Paramachairodus ogygia* (Felidae, Machairodontinae) from the Late Miocene of Spain. J Zool 268:243-254. doi:10.1111/j.1469-7998.2005.00032.x

Salesa MJ, Antón M, Turner A, Alcalá L, Montoya P, Morales J (2010a) Systematic revision of the late Miocene sabretoothed felid *Paramachaerodus* in Spain. Palaeontology 53(6):1369-1391. doi:10.1111/j.1475-4983.2010.01013.x

Salesa MJ, Antón M, Turner A, Morales J (2010b) Functional anatomy of the forelimb in *Promegantereon ogygia* (Felidae, Machairodontinae, Smilodontini) from the late Miocene of Spain and the origins of the sabertoothed felid model. J Anat 216(3):381-96. doi: 10.1111/j.1469-7580.2009.01178.x

Salesa MJ, Montoya P, Alcalá L, Morales J (2003) El género *Paramachairodus* Pilgrim, 1913 (Felidae, Machairodontinae) en el Mioceno superior español. Coloquios de Paleontología 1:603–615

Salesa MJ, Pesquero MD, Siliceo G, Antón M, Alcalá L, Morales J (2012a) A rich community of Felidae (Mammalia, Carnivora) from the late Miocene (Turolian, MN 13) site of Las Casiones (Villalba Baja, Teruel, Spain). J Vertebr Paleontol 2(3):658–676. doi:10.1080/02724634.2012.649816

Sardella R (1998) The Plio-Pleistocene Old World dirk-toothed cat *Megantereon* ex gr. *cultridens* (Mammalia, Felidae, Machairodontinae), with comments on taxonomy, origin and evolution. Neues Jahrb Geol Paläontol Monatsh 207(1):1-36

Schlager S (2017) Morpho and Rvcg–Shape Analysis in R: R-Packages for geometric morphometrics, shape analysis and surface manipulations. In: Zheng G, Li S, Székeli G (eds.) Statistical Shape and Deformation Analysis. Elsevier, London, pp 217-256

Schaeffer J, Benton MJ, Rayfield EJ, Stubbs TL (2019) Morphological disparity in theropod jaws: comparing discrete characters and geometric morphometrics. Palaeontology 63(2):283-299. doi:10.1111/pala.12455

Segura V (2015) A three-dimensional skull ontogeny in the bobcat (*Lynx rufus*) (Carnivora: Felidae): a comparison with other carnivores. Can J Zool 93(3):225–237

Siliceo G, Salesa MJ, Antón M, Monescillo MF, Morales J (2014) *Promegantereon ogygia* (Felidae, Machairodontinae, Smilodontini) from the Vallesian (late Miocene, MN 10) of Spain: morphological and functional differences in two noncontemporary populations. J Vertebr Paleontol 34(2):407-418. doi:10.1080/02724634.2013.812099

Slater GJ, Van Valkenburgh B (2009) Allometry and performance: the evolution of skull form and function in felids. J Evol Biol 22(11):2278-2287. doi:10.1111/j.1420-9101.2009.01845.x

Stubbs TL, Pierce SE, Rayfield EJ, Anderson PS (2013) Morphological and biomechanical disparity of crocodile-line archosaurs following the end-Triassic extinction. Proc R Soc 280:20131940. doi:10.1098/rspb.2013.1940

Tseng ZJ, Grohé C, Flynn JJ (2016) A unique feeding strategy of the extinct marine mammal *Kolponomos*: convergence on sabretooths and sea otters. Proc R Soc 283:20160044.. doi:10.1098/rspb.2016.0044

Turner A, Antón M (1997) The Big Cats and Their Fossil Relatives. Columbia University Press, New York

Turner A, Antón M, Salesa MJ, Morales J (2011) Changing ideas about the evolution and functional morphology of machairodontine felids. Estud Geol 67(2):255–276

Wallace SC, Hulbert RC Jr (2013) A new machairodontine from the Palmetto Fauna (early Pliocene) of Florida, with comments on the origin of the Smilodontini (Mammalia, Carnivora, Felidae). PloS One 8(3):e56173. doi:10.1371/journal.pone.0056173

Werdelin L, Flink T (2018) The phylogenetic context of *Smilodon*. In: Werdelin L, McDonald HG, Shaw CA (eds) *Smilodon* the Iconic Sabertooth. John Hopkins university press, Baltimore, 14–29

Werdelin L, Lewis ME (2000) Carnivora from the South Turkwel hominid site, northern Kenya. J Paleontol 74(6):1173–1180

White JA, McDonald HG, Anderson E, Soiset JM (1984) Lava blisters as carnivore traps. Carnegie Mus Nat Hist Special Publi 8:241–256

Werdelin L, Yamaguchi N, Johnson E, Brien SJO (2010) Phylogeny and evolution of cats (Felidae). In: Macdonald D, Loveridge A (eds) Biology and Conservation of Wild Felids. Oxford University Press, Oxford, 59–82

Wiley DF, Amenta N, Alcantara DA, Ghosh D, Kill YJ, Delson E, Harcourt-Smith W, Rohlf FJ, St. John K, Hamann B (2005) Evolutionary morphing. Institute for Data Analysis and Visualization, University of California Davis. https://escholarship.org/uc/item/4k5991zk. Accessed 23 March 2019